ADVANCED BIOLOGY
www.advanced-bio.com

Lithium Directs Embryonic Stem Cell Differentiation Into Hemangioblast-Like Cells

Hayk Mnatsakanyan, Manuel Salmeron-Sanchez, and Patricia Rico**

Definitive hematopoietic stem cells (HSCs) derive from specialized regions of the endothelium known as the hemogenic endothelium (HE) during embryonic developmental processes. This knowledge opens up new possibilities for designing new strategies to obtain HSCs in vitro from pluripotent stem cells (PSCs). Previous advances in this field show that the Wnt/β-catenin signaling pathway plays a crucial role in PSC-derived HSC formation. In this work, lithium, a GSK3 inhibitor, is identified as an element capable of stabilizing β-catenin and inducing embryonic stem cells (ESCs) differentiation in hemangioblast-like cells, highly consistent with the role of Wnt agonists on ESC differentiation. ESCs treated with 10 mM lithium express CD31+, SCA-1+, Nkx2-5+, CD34+, and FLK1+ cells characteristic of the hemangioblast cells that precede HE development. However, 10 mM Li treated cells remain arrested in a hemangioblast-like phase, which switched into the expression of HE markers after stimulation with maturation medium. The ability of lithium-treated ESCs to further derive into HE is confirmed after defined maturation, resulting in a rapid increase in cells positive for the HE markers RUNX1 and SOX17. The results represent a novel strategy for generating HSC precursors in vitro as a multipotent source of stem cells for blood disease therapies.

1. Introduction

Hematopoietic stem cells (HSCs) are multipotent stem cells capable of self-renewal and differentiation.[1] They are the main source of the precursors of all classes of blood cells.[2] Image tracing experiments have supported the idea that definitive HSCs arise from specialized vascular endothelial cells that acquire blood-forming potential (hemogenic endothelium, HE).[3–5] HE specification responds to the need to develop a functional circulatory system to provide oxygen and nutrients to all types of tissue during embryogenesis.[4] During the embryonic development, both blood vessels and HE cells arise simultaneously at the same anatomical site from the same mesodermal precursor, the hemangioblast (HB).[6] Depending on the signaling context, these cells can contribute to either vascular smooth muscle, endothelium, or HE.[7]

HE and definitive HSC development from pluripotent stem cells (PSCs) are driven by Wnt/β-catenin signaling, activated by either Wnt or Wnt agonists such as GSK3 inhibitors.[3,8] Previous studies on CHIR99021 have shown that this pharmacological GSK3 inhibitor is capable of stabilizing β-catenin and promoting its transcriptional activity[9,10] and thus inducing HE formation. The activation of the Wnt pathway by inhibiting GSK3 using CHIR99021 followed by stimulation of the vascular endothelial growth factor (VEGF) further induces the differentiation of PSCs to HE and subsequently to HSCs.[11] Lithium is another well-defined GSK3 inhibitor[12] and has been used for the treatment of bipolar disorder for decades.[12] However, its inhibiting effect on GSK3 in embryonic stem cells (ESCs) differentiation is somewhat controversial. Previous studies suggested that murine ESCs treated with lithium differentiate towards neural cells[13] instead of mesodermal lineage.

Although considerable efforts have been made to direct PSC fate towards hematopoietic lineages, the efficient synthesis of HSC precursors needs a deeper understanding of the molecular mechanisms that control HSCs fate.[14] HSCs are now widely used in clinical transplantations as a cancer therapy and for other blood or immune disorders.[14] Unfortunately, their use is restricted due to the present limited primary HSC sources and questions of donor/receptor compatibility,[14,15] so that alternative methods are needed to overcome these limitations. PSC-derived HSCs can thus be considered as a major breakthrough in this regard, even though the low efficiency in generating hematopoietic cells from PSCs is one of the major hurdles to this approach.[14] The differentiation of PSCs into HSCs follows multiple steps, beginning with the differentiation of PSCs into the mesodermal lineage. Then, mesodermal cells under appropriate conditions become HB cells, characterized by the expression of VEGF receptor 2 (Flk1) and Brachyury (T).[7] HB possesses the potential to derive from both endothelial and HE cells.

Dr. H. Mnatsakanyan, Prof. M. Salmerón-Sánchez, Dr. P. Rico
Center for Biomaterials and Tissue Engineering (CBIT)
Universitat Politècnica de València
Camino de Vera s/n, Valencia 46022, Spain
E-mail: Manuel.Salmeron-Sanchez@glasgow.ac.uk; parico@upvnet.upv.es
Prof. M. Salmerón-Sánchez, Dr. P. Rico
Biomedical Research Networking Center in Bioengineering Biomaterials and Nanomedicine (CIBER-BBN)
Instituto de Salud Carlos III
C/ Monforte de Lemos 3-5 Pabellón 11, Madrid 28029, Spain
Prof. M. Salmerón-Sánchez
Centre for the Cellular Microenvironment
University of Glasgow
Glasgow G12 8LT, United Kingdom
The ORCID identification number(s) for the author(s) of this article can be found under https://doi.org/10.1002/adbi.202000569.

DOI: 10.1002/adbi.202000569

Regarding HE development from HB cells, Runx1 has been described as a master regulator of this process. In the absence of Runx1 expression, HB cells lose their potential to derive into HSCs.[16] The complexity of HSCs generation during embryogenesis highlights the importance of the intricate multistep process controlling the formation of blood cells in vitro efficiently.

Here we define the lithium-activated mechanisms on murine ESC self-renewal and differentiation, focusing on lithium-mediated inhibition of GSK3β activity and how this effect can modulate both β-catenin expression and nuclear translocation, driving ESC differentiation towards HSC precursors. We demonstrate the ability of these lithium-treated ESCs to differentiate into HB-like cells and further derive into HE after defined maturation. Thus, our results demonstrate a novel, simple and efficient strategy for generating efficiently both HB and HE endothelial cells from PSCs without using cytokines or complex cell culture cocktails.

2. Results

2.1. Li^+ Effects on ESC Proliferation and GSK3β Phosphorylation are Dose-Dependent

Concentrations of Li^+ above 2 mM have shown both cytotoxic and anti-proliferative effects in other cell types.[17] ESCs were cultured with increasing concentrations of Li^+ for 3 days to determine the cytotoxicity of Li^+ on mouse PSCs. 20 mM Li^+ was toxic for ESCs after 1 day. The number of ESC colonies was considerably fewer than in the other conditions (Figure S1, Supporting Information). ESCs treated with 5 and 10 mM Li^+ showed both lower cell density (Figure S1, Supporting Information) and DNA concentration than 2 mM Li^+ and cells grown in BM (**Figure 1**a) after 1 day of culture, indicating that high concentrations of Li^+ (below 20 mM) reduce cell proliferation without affecting cell viability.

In order to clarify the mechanism by which Li^+ reduces ESC proliferation, we studied P53-mediated regulation of the cell cycle via $P27^{Kip1}$.[18] It has previously been found that 10 mM Li^+ activates P53 and reduces cell proliferation.[19] We analyzed the number of mitotic cells and the expression of $P27^{Kip1}$ in ESCs cultured in BM and medium supplemented with 10 mM Li^+. The number of mitotic cells was reduced in the presence of 10 mM Li^+ after 24 h (Figure 1b), which agrees with the DNA concentrations shown in Figure 1a. Regarding the $P27^{Kip1}$ expression, ESCs treated with 10 mM Li^+ showed higher nuclear staining regardless of colony density (Figure 1c, 1d, 1f), whereas those cultured in BM showed a monotonical increase of $P27^{Kip1}$ according to colony density (Figure 1e and Figure S2, Supporting Information). These results show that the presence of Li^+ promotes $P27^{Kip1}$ expression and arrests the ESC cell cycle.

We next evaluated the Li^+-mediated phosphorylation of two key PSC regulators: GSK3β and its post-translational regulator AKT[10] (Figure 1g). Results indicated that GSK3β phosphorylation did not undergo significant changes after 4 and 24 h in cells cultured with LIF and BM. However, for both time points, ESCs supplemented with Li^+ showed higher dose-dependent GSK3β phosphorylation. For AKT phosphorylation, no significant differences were observed in Li^+-treated cells, showing similar pAKT/AKT ratio values to those of BM and LIF-cultured cells, suggesting that Li^+ has no significant effect on AKT phosphorylation (Figure 1g).

2.2. Li^+ Enhances β-Catenin Expression and Nuclear Translocation Directing ESC Differentiation into Mesodermal Lineage

Although β-catenin activity has been shown to be essential for maintaining ESC integrity,[20] excessive β-catenin accumulation in the nucleus leads to the expression of Cdx1, Cdx2, and Brachyury/T, genes implicated in lineage differentiation.[21] To study how Li^+ affects β-catenin expression and its subcellular distribution, we assessed the nuclear accumulation of β-catenin and GSK3β phosphorylation by immunofluorescence and western blot (**Figure 2**).

As expected, after 1 day of culture GSK3β phosphorylation was significantly higher in ESCs treated with 10 mM Li^+ (as shown in Figure 1g) with no significant differences in terms of β-catenin expression (Figure 2a). After 3 days, the pGSK3β/GSK3β ratio increased monotonically in Li^+-treated cells, with reduced non-phosphorylated GSK3β expression, whilst β-catenin expression increased. Immunofluorescence analyses showed increased accumulation of β-catenin in the nuclei of ESCs treated with 10 mM Li^+ after 3 days (Figure 2b). To confirm whether nuclear localization of β-catenin was related to the activation of its transcriptional targets involved in PSC differentiation (Figure 2c), we analyzed β-catenin binding with the Cdx2 promoter by ChIP on PCR. Only ESCs treated with 10 mM Li^+ showed amplification in this promoter region (Figure 2c).

To further demonstrate β-catenin transcriptional activity, we analyzed the differential expression of two of its target genes: Brachyury/T and Cdx2. Both transcription factors are key regulators of the early mesodermal commitment in PSCs.[21] qPCR amplification showed a significantly higher expression of both Brachyury/T and Cdx2 in ESCs treated with 10 mM Li^+ (Figure 2d). Results indicate that high concentrations of Li^+ can induce ESC differentiation towards the mesodermal lineage and also that 10 mM Li^+ can efficiently inhibit the β-catenin destruction complex.

2.3. High Concentrations of Li^+ Promote Nuclear GKS3β Accumulation

The activity of GSK3β is not just limited to the control of β-catenin degradation. The protein kinase GSK3β can be found in different subcellular localizations such as cytosol, mitochondria, and nucleus.[22] Inside the nucleus, GSK3β targets several transcription factors, such as P53,[22] regulating their activity (**Figure 3**a). To determine whether Li^+ affects GSK3β subcellular localization, we quantified the nuclear intensity of immunostained GSK3β (Figure 3b). Only ESCs treated with 10 mM Li^+ showed a significant increase in nuclear GSK3β after 3 days of culture. The increase in nuclear accumulation of GSK3β, together with the reduced ESCs proliferation exposed to 10 mM Li^+, strongly suggest that GSK3β is activating P53. The transcriptional network activated by both β-catenin and

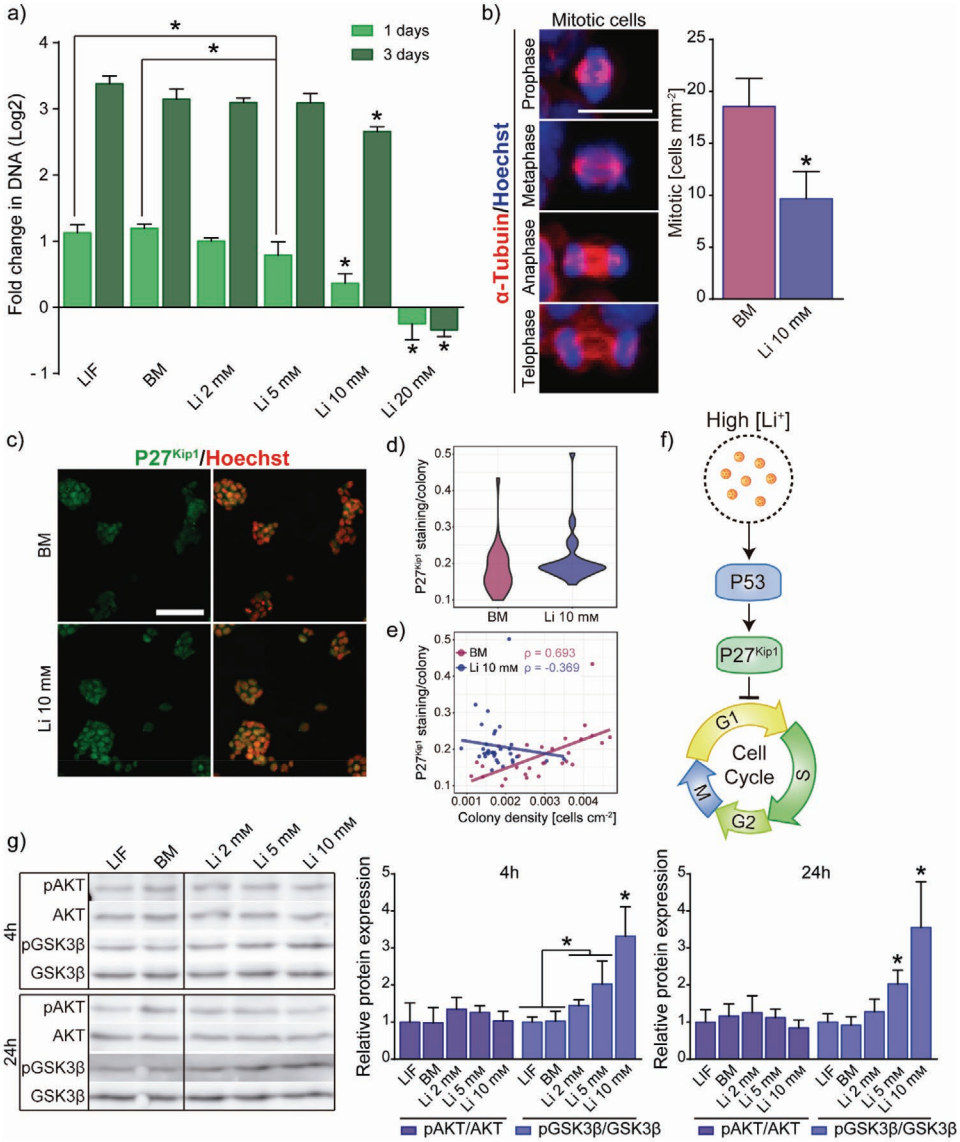

Figure 1. Role of Li^+ on ESC proliferation and GSK3β phosphorylation. a) DNA concentration in ESCs treated with increasing concentrations of Li^+ after 1 and 3 days ($n = 4$). Scale bar: 20 µm. b) Analysis of mitotic cells in ESCs cultured in BM and medium supplemented with 10 mM Li^+ after 24 h ($n = 5$). c) Immunofluorescence detection of $P27^{Kip7}$ in ESCs cultured for 24 h in BM and medium supplemented with 10 mM Li^+. Scale bar: 200 µm. d) Quantification of the nuclear accumulation of $P27^{Kip1}$ per ESCs colony after 24 h. e) Correlation between the nuclear accumulation of $P27^{Kip1}$ in ESC colonies and the colony density. Spearman correlation ρ value was determined. f) Representation of the mechanisms activated by 10 mM Li^+ to inhibit cell cycle progression. g) Western blot analysis of GSK3β (S9) and AKT (S473) phosphorylation in ESCs treated with increasing concentrations of Li^+ after 4 and 24 h of culture. GAPDH was used as a loading control ($n = 4$). Graphs show mean ± SD ($^*p < 0.05$).

P53 revealed a great number of genes associated with the mesodermal and HE lineages regulated by these transcription factors (Figure 3c). Immunofluorescence assays of HSC precursor markers SCA-1, CD31, RUNX1, and FLK1 indicated their presence only after treatment of ESCs with 10 mM Li for 3 days. These results are in concordance with the higher gene expression levels of Brachyury/T obtained after 10 mM Li^+ treatment showed in Figure 2d. The combined expression of Brachyury/T, together with FLK1 suggests that 10 mM Li^+ promotes hemangioblast development from ESCs.

2.4. High Concentrations of Li^+ Promote ESC Differentiation Into Hemangioblast (HG) Like Cells

Previous studies have shown that GSK3β inhibition induces HE development from ESCs.[8,11] Next, we studied whether continued exposure to 2 and 10 mM Li^+ drives ESC differentiation into HE after 6 days of culture. We analyzed pluripotency and HE-specific markers by immunofluorescence and qPCR. The ratio of OCT4 and SOX2 (pluripotency markers) positive cells indicated that ESCs treated with 10 mM Li^+

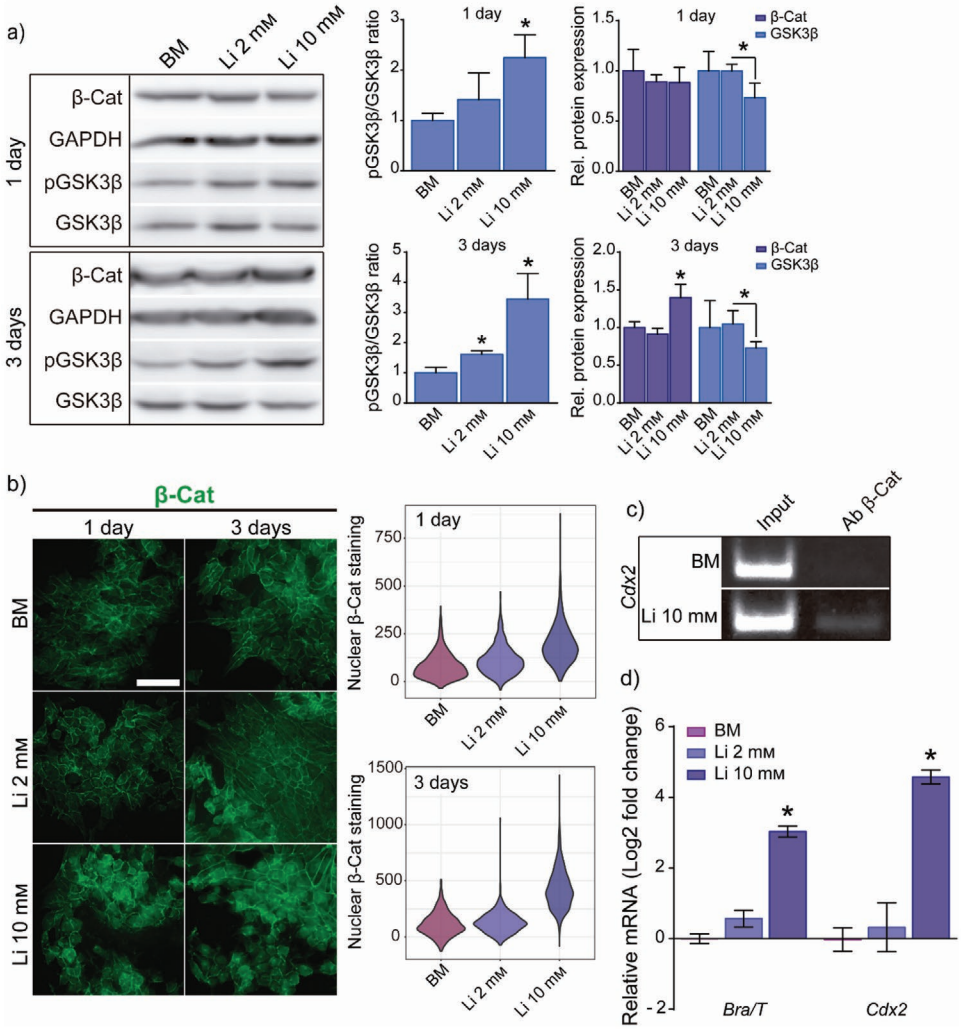

Figure 2. GSK3β activity, β-catenin expression, and subcellular localization in Li^+-treated cells. a) Western blot analysis of β-catenin expression and pGSK3β/GSK3β ratio in ESCs cultured for 1 and 3 days with different Li^+ concentrations. GAPDH was used as a loading control protein ($n = 4$). b) Quantification of β-catenin immunostaining after 1 and 3 days of culture. ($n > 1000$ random nuclei. Scale bar 50 µm. c) ChIP on PCR assay of β-catenin binding region in Cdx2 gene. d) qPCR evaluation of mesoderm markers Brachyury/T and Cdx2 expression in ESCs cultured with different concentrations of Li^+ after 3 days of culture. GAPDH was used as housekeeping gene ($n = 4$). Graphs show mean ± SD ($^*p < 0.05$).

showed accelerated differentiation (Figure S3a, Supporting Information). After 6 days of culture, HE progenitor markers SCA-1, CD31, CD34, VE-cadherin, and FLK1 were highly expressed in ESCs cultured with 10 mM Li^+ (**Figure 4**). We found that the resulting population of 10 mM Li^+-treated cells consisted of a combination of either SCA-1+ cells, CD31+ cells, or both (Figure 4a, 4b). We further found that continued treatment for 6 days with 10 mM Li^+ was necessary to reach a significant population of SCA-1+ and CD31+ cells (Figure S3b, Supporting Information). When 10 mM Li^+ was removed from the culture medium (3D-Li 10 mM), the effect on proliferation disappeared for the next 3 days, with significantly higher cell density than in ESCs treated for all 6 days with 10 mM Li^+, and thus reversing lithium's effect of arresting cell cycle progression. Regarding the expression of RUNX1, we observed some RUNX1+ cells in 10 mM Li^+-treated cells after 6 days of culture (Figure 4e). However, the ratio of RUNX1+ did not vary significantly from 3 to 6 days of culture (Figure 4f). Besides, the expression of SOX17, which is characteristic of HE cells,[23] was not significantly appreciable, and only RUNX1+ cells showed SOX17 expression (Figure 4e).

We further analyzed the expression of HG and cardiac mesoderm markers Nkx2-5 and Gata4 after 6 days. Nkx2-5 was only overexpressed in ESCs treated with 10 mM Li^+ (Figure 4g) while Gata4 did not show significant differences between BM and 10 mM Li^+-treated ESCs. The expression of Nkx2-5 and the absence of Gata4 expression indicate that there is no cardiac mesodermal differentiation and suggest that ESCs exposed to 10 mM Li^+ differentiated to HG-like cells. This evidence is supported by the low number of cells expressing HE markers such as SOX17 and RUNX1 (Figure 4e).

In silico analysis (Figure 3c) suggests that the transcriptional activity of P53, activated by GSK3β nuclear translocation

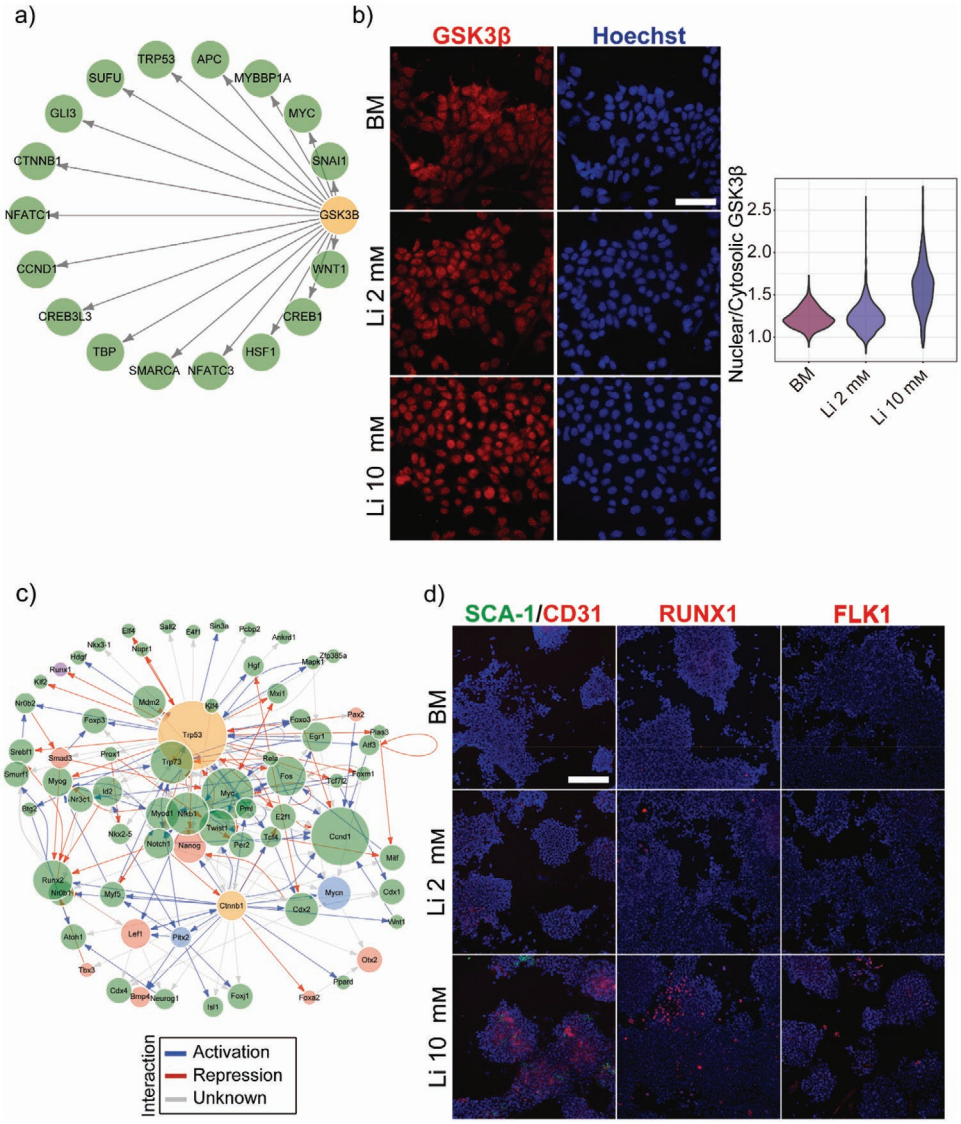

Figure 3. Effects of Li^+ in GSK3β subcellular localization and ESCs differentiation. a) In silico analysis of transcription factors that interact with the protein kinase GSK3β. Interactions were obtained from STRING database. V11. Only interactions with a combined score equal or higher to 900 were considered. b) Quantification of nuclear staining of GSK3β after 3 days of culture (n > 500 random nuclei). Scale bar 50 µm. c) In silico analysis of transcriptional targets of P53 (Tpr53) and β-Catenin (Ctnnb1) related to PSC differentiation into mesodermal lineage (Red), HSCs precursors (Blue), and HE (Purple). Data was obtained from TRRUST database (V2). d) Immunofluorescence analysis of HE markers (SCA-1, CD31, FLK1, and RUNX1) in ESCs cultured for 3 days with different concentrations of Li^+. Scale bar 200 µm.

via Li^+, could hinder the expression of RUNX1. The expression of RUNX1 has been described as crucial for the HG specification into HE.[24] Following, we investigated whether a high concentration of Li^+ is arresting ESCs exposed to 10 mM Li^+ for 6 days in HG-like cells. After 6 days, we switched the differentiation medium by the maturation medium (N2B27) and cultured cells for an additional 3 days (6 d + 3 d N2B27). As a control, we used ESCs exposed to 10 mM Li^+ for 9 days. Our results indicated that the removal of 10 mM Li^+ increased the number of SOX17+ cells after 3 days (Figure 4h), supporting the hypothesis that Li^+ must be removed to enable the transition from HB to HE.

2.5. Li^+-Induced ESCs-Derived Hemangioblast-Like Cells Can be Maturated to Obtain HE Cells

Definitive HSCs deriving from HE arise from a subset of the population characterized by the expression of both RUNX1+ and SCA-1+ cells.[25,26] We observed that after 6 days of culture with 10 mM Li^+, ESCs successfully differentiated into SCA-1+ cells and showed a faint expression of RUNX1 and nuclear β-catenin (Figure S4, Supporting Information). To further investigate the potential of SCA-1+ cells derived from ESCs to differentiate into HE, we induced them to differentiate under maturation medium N2B27 for 11 days (**Figure 5**a). The expression of HE

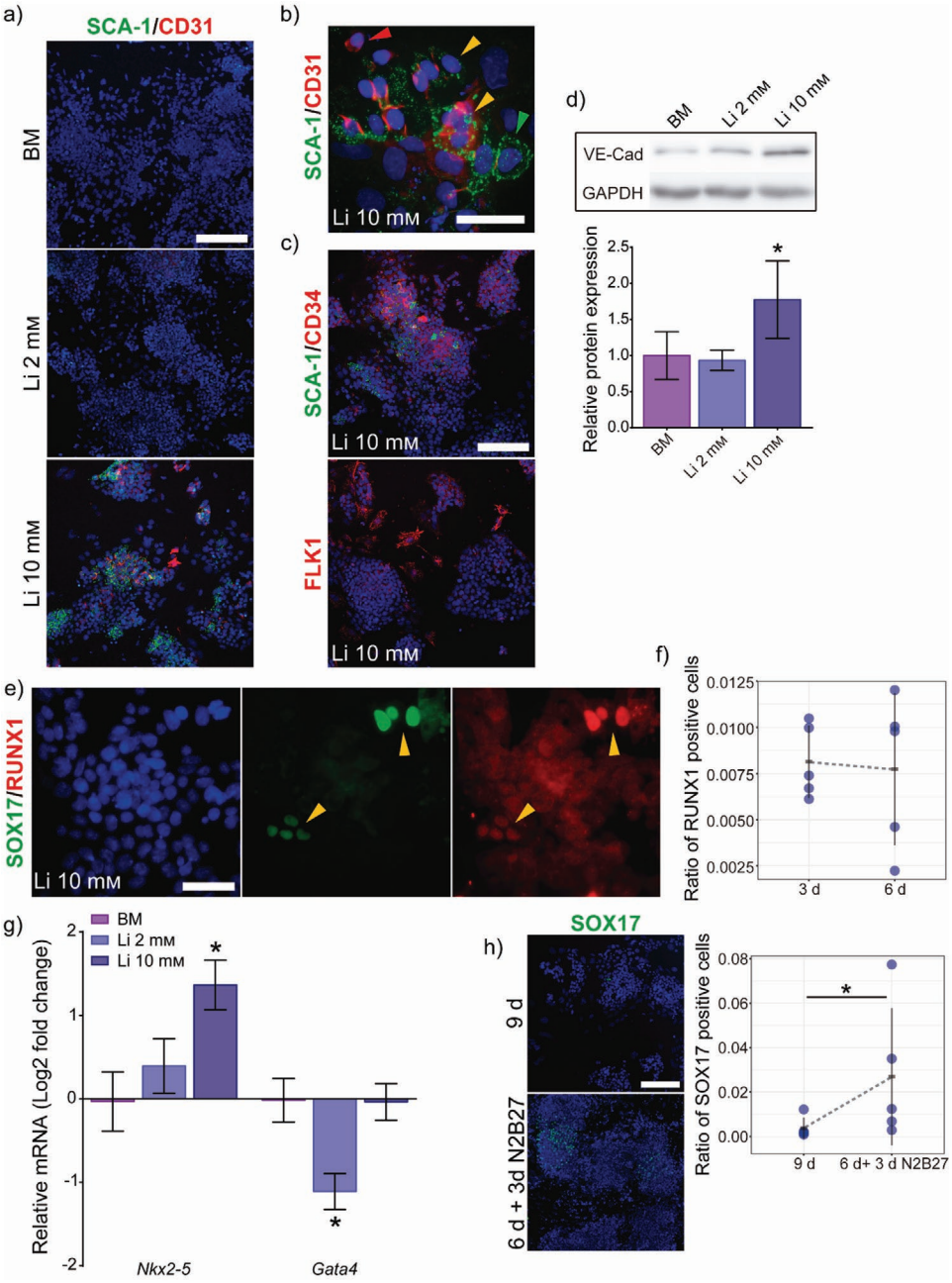

Figure 4. Effects of Li^+ on ESCs cultured for 6 days in monolayer. a) Immunofluorescence analysis of HE markers (SCA-1 and CD31) in ESCs cultured for 6 days with different concentrations of Li^+. Scale bar 200 µm. b) Representative images of ESCs cultured with 10 mM Li^+, with a variety of coexisting CD31+ (red arrow), SCA-1+ (green arrow), and CD31+/SCA-1+ (yellow arrow) cells. Scale bar 50 µm. c) Immunofluorescence analysis of HE markers (FLK1, SCA-1, and CD34) in ESCs cultured for 6 days with different concentrations of Li^+. Scale bar 200 µm. d) Western blot analysis of the expression of VE-cadherin after 6 days of culture in ESCs treated with different concentrations of Li^+. GAPDH was used as a loading control protein ($n = 4$). e) Immunofluorescence analysis of HE markers RUNX1 and SOX17 after 6 days of culture in ESCs treated with 10 mM Li^+ (yellow arrow indicates cells expressing both markers). Scale bar 50 µm. f) Quantification of the ratio of RUNX1 positive cells in ESCs treated with 10 mM Li^+ after 3 and 6 days of culture ($n = 5$). g) qPCR analysis of HE markers (Nkx2-5 and Gata4) in ESCs cultured for 6 days with different concentrations of Li^+ ($n = 4$). h) Quantification of the ratio of SOX17 positive cells in ESCs treated with 10 mM Li^+ for 6 days and subsequently maturated in N2B27 medium for an additional 3 days. As a control, 10 mM Li^+ containing medium was maintained for those additional 3 days ($n = 5$). Scale bar 200 µm. Graphs show mean ± SD (*$p < 0.05$).

markers (SCA-1, CD31, CD34, RUNX1, and SOX17) was analyzed by immunostaining after 5 and 11 days of maturation (Figure 5). After 5 days, HE markers RUNX1 and SOX17 were upregulated in the ESCs pre-treated with 10 mM Li^+, observing an increasing number of cells co-expressing both markers (Figure 5b, 5c). These cells begin to appear spatially close to SCA-1-expressing colonies (Figure 5b and Figure S5b, Supporting Information), suggesting that their origin lies in SCA-1+

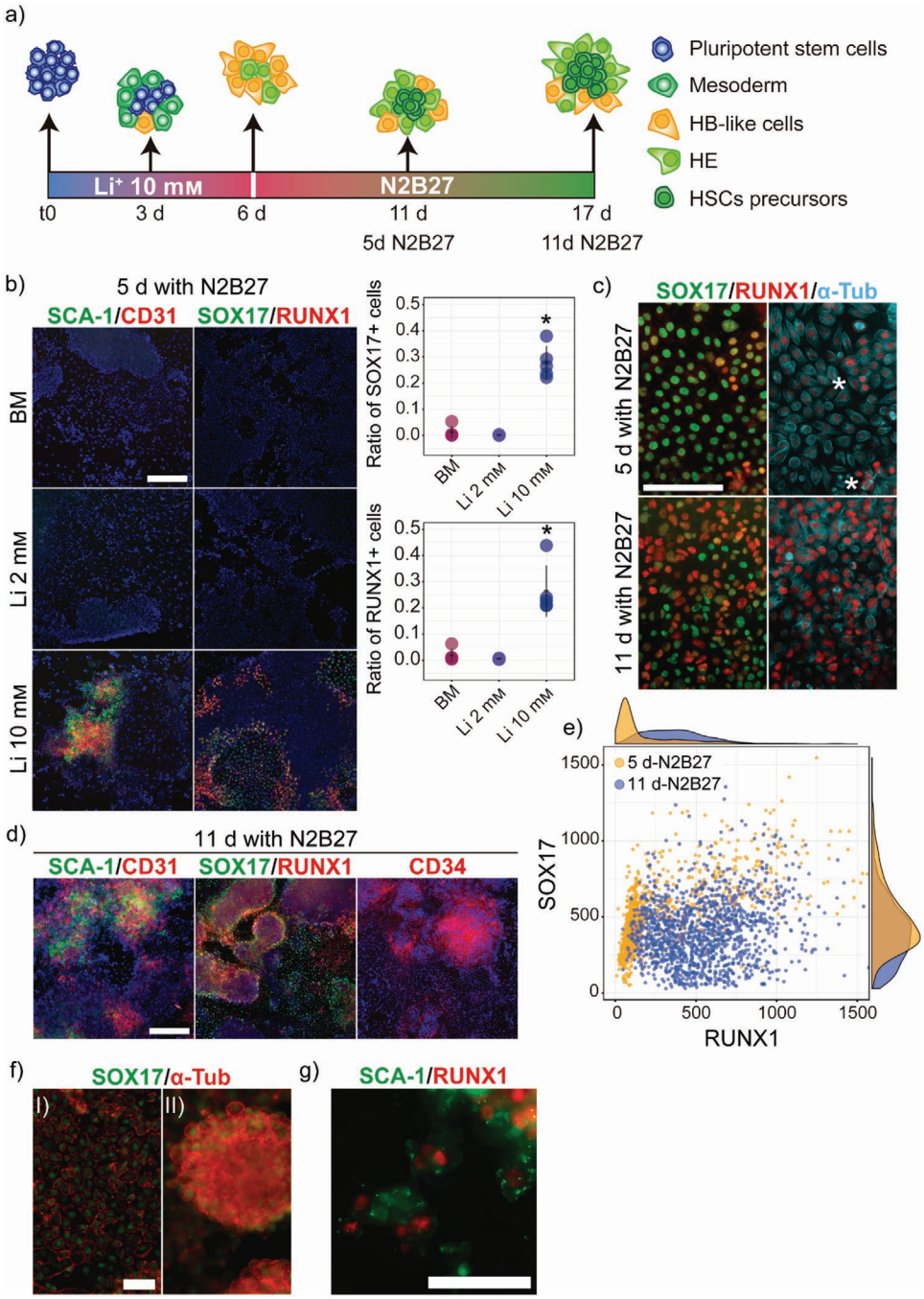

Figure 5. Maturation of hemangioblast-like cells derived from ESCs treated with 10 mM Li^+ into HE. a) Experimental set up for differentiation of ESCs in the presence of 10 mM Li^+ for 6 days and then maturated in HSC precursors for 11 days under differentiation conditions (maturation medium N2B27). b) Immunofluorescence detection of HE markers (SCA-1, CD31, SOX17, and RUNX1) in ESCs pre-cultured for 6 days in the presence of different concentrations of Li^+ and then maturated for 5 days in N2B27. The ratio of RUNX1+ and SOX17+ cells was quantified by image analysis ($n = 5$). Scale bar 200 µm. c) Immunofluorescence images of the evolution of SOX17 and RUNX1 expression during the maturation of ESCs pre-cultured with 10 mM Li^+. Cell clamping is indicated by white asterisks. Scale bar 200 µm. d) Immunofluorescence detection of HE markers (SCA-1, CD31, CD34, RUNX1, and SOX17) in ESCs pre-cultured for 6 days with 10 mM Li^+ and then maturated for 11 days in N2B27. Scale bar 200 µm. e) Analysis of the nuclear accumulation of RUNX1 and SOX17 during the maturation of ESCs pre-cultured for 6 days with 10 mM Li^+ and then maturated for 5 and 11 days in N2B27 maturation medium ($n > 1000$ nuclei). f) Immunofluorescence analysis of the morphology of the cells expressing Sox17 (hemogenic endothelial and HSC precursor marker) after 11 days of maturation. Scale bar 50 µm. g) Immunostaining of hemogenic endothelial-like cells obtained after 11 days of maturation that co-express both RUNX1 and SCA-1. Scale bar 50 µm. Graphs show mean ± SD (*$p < 0.05$).

cells. These results are consistent with the fact that definitive HSCs arise from HE expressing both SCA-1 and RUNX1.

Bright-field images showed that ESCs pre-treated with 10 mM Li^+ and matured for 7 days possessed both endothelial-like cell and clustered and rounded cell morphologies (Figure S5a, Supporting Information), reinforcing the idea of HE commitment of HB-like cells. After 11 days, cell morphologies of ESCs pre-cultured in BM or 2 mM Li^+ and those treated with 10 mM Li^+ were clearly different. While 10 mM Li^+-treated ESCs showed a significant population of rounded cells over endothelial-like colonies, the other conditions showed many neural-like cells (Figure S5a, Supporting Information). The CD31+, CD34+, SCA-1+, RUNX1+, and SOX17+ cell populations increased even more in ESCs pre-treated with 10 mM Li^+ after 11 days in a maturation medium, with a large number of clamped colonies (Figure 5d, 5f and Figure S5c, Supporting Information). Indeed, after 11 days, the RUNX1/SOX17 ratio in cells co-expressing RUNX1 and SOX17 increased compared with those of cells after 5 days (Figure 5e). After 11 days of culture under maturation conditions, we observed a gradual change in cell morphology. The appearance of clusters composed of rounded cells expressing SOX17 supported the idea of HE differentiation and the potential to originate endothelial to hematopoietic cell transition (EHT, Figure 5f). In addition to previous evidence, HB-like cells maturated for 11 days showed a great number of cells co-expressing RUNX1 and SCA-1 markers (Figure 5g). Even though the resulting populations of HB and HE-like cells were clearly heterogeneous, these results suggest that we obtained HE-like cells with the potential to differentiate into definitive HSCs.

To test our hypothesis based on lithium's capacity to induce ESC differentiation into HB-like cells and further maturation into HE, we further analyzed relevant parameters after culturing ESC in suspension (Figure S6, Supporting Information). We obtained spheroids showing that Li^+ successfully induced ESC differentiation into HB-like cells and subsequently to HE even in suspension.

3. Discussion

GSK3β activity is an essential molecular cue controlling ESCs' fate.[21,27] Previous reports have indicated that GSK3 activity is related to both ESC self-renewal/differentiation[21] and β-catenin inhibition.[10] Other works related to Li^+ effects suggest that high concentrations of Li^+ inhibited ESC differentiation towards cardiac lineage, favoring neural differentiation.[13] Despite these reports, we did not find any neural (Figure S5a, Supporting Information) or cardiac (Figure 4g) differentiation after using 10 mM Li^+. In fact, we have found that the presence 10 mM Li^+ reduced ESCs' pluripotency potential diminishing the ratio of OCT4+ cells (Figure S3a, Supporting Information). Besides, the continued exposure of ESCs to 10 mM Li^+ strongly inhibited (phosphorylated) GSK3β and induced β-catenin transcriptional activation (Figure 2), giving rise to mesoderm development (Figure 2) and subsequent HB specification (Figures 2 and 3), in ESCs cultured in both, monolayer (Figures 3 and 4) and in suspension (Figure S6, Supporting Information).

Our findings are supported by other studies based on the use of GSK3β inhibitors.[11] The activation of Wnt signaling by either Wnt or GSK3β inhibitors has shown to induce HE differentiation in ESCs.[8,11,12] Here, we demonstrate that after 6 days of culture, initial ESC colonies expressed SCA-1, CD31, CD34, FLK1, VE-cadherin, Nkx2-5, and low levels of RUNX1 (Figure 3 and Figure S4, Supporting Information). These markers are characteristic of mesodermal cells with the potential to develop HSCs.[3,28] Furthermore, in silico analysis predicts that the combined activity of both P53 and β-catenin activated by 10 mM Li^+ could target many genes related to mesodermal lineages differentiation (Figure 3c) and HSCs precursors development (Figure 3c). Even though Nkx2-5 is a master regulator of cardiogenesis,[29] its expression has also been found in HB cells.[28] In silico analysis also predicted that the P53 activation by 10 mM Li^+[19] could hinder the development of mature HE cells because of the transcriptional inactivation of Runx1 (Figure 2c), which is essential for the development of both HSCs and HE.[30,31] Even though more experiments would be necessary to confirm this hypothesis, it explains the faint staining of RUNX1 observed after 6 days in the presence of 10 mM Li^+ and the rapid increase when the medium was replaced by the maturation medium (without Li^+). In addition to that, P53 mediated repression of RUNX1 also explains why once Li^+ was removed from the culture medium, HB-like cells showed a burst of SOX17 expressing cells (Figure 4h). Thus, our results suggest that 10 mM Li^+ induces ESCs differentiation into HB-like cells and maintains them arrested in that stage.

The capability of HB-like cells obtained with 10 mM of Li^+ to derive into HE was confirmed after their defined maturation (Figure 5). After 11 days in N2B27 maturation medium, we found rounded cells expressing RUNX1 and SOX17. As SOX17 expression is a feature of HE cells[23] and fetal HSCs before the acquisition of the adult phenotype,[32] HSCs developed from PSCs can be expected to share many characteristics with fetal HSCs because of their embryonic-like origin.[33] Furthermore, after 11 days in the maturation medium, the ratio between RUNX1/SOX17 was significantly higher (Figure 5c, 5e) than the values observed after 5 days. As SOX17 has been reported to impair RUNX1 transcriptional activity, its downregulation is necessary for EHT.[30] These results were reinforced by the changes in the cell morphologies; we observed RUNX1/SOX17 expression in clumped and rounded cells (Figure 5c, 5f), while RUNX1 expression significantly increased respect the expression of SOX17 (Figure 5e), enabling the subsequent step of EHT. Our results showed that the population of HE cells obtained after 11 days of maturation was highly heterogeneous. However, it is noteworthy that we observed many RUNX1+/SCA-1+ cells. This feature is remarkable since this subset of the population has been described as the precursors of definitive HSCs,[25] supporting previous results reporting the transition from HB-like cells to HE-like cells.

Altogether, we have defined the mechanisms activated by lithium on murine ESC self-renewal and differentiation. Li^+ can thus be regarded as a powerful molecule capable of efficiently activating the β-catenin transcription factor involved in the generation of HSCs precursors from ESCs. We have also shown the ability of these lithium-treated ESCs to further derive into HE cells after defined maturation, confirming the potential of

Li^+ to direct ESCs differentiation into HSCs precursors. These results represent a promising strategy for the successful generation of blood cells in vitro, allowing to overcome the first obstacle to obtain HSCs, the generation of a wide population of HB and HE precursors for biomedical blood applications.

4. Experimental Section

ESCs Culture: Murine ESC (D3-ESCs, ATCC) were cultured in feeder-free conditions using ESCs basal medium (BM) composed by Dulbecco's modified Eagle's medium (DMEM) high glucose (Lonza) supplemented with 10% Knockout Serum Replacement (KSR, ThermoFisher), 1% fetal bovine serum (Gibco), 1% 100X Nucleosides (Millipore), 1% L-glutamine (Sigma-Aldrich), 1% non-essential amino acids (Sigma-Aldrich), 1% 100X penicillin/streptomycin (P/S, ThermoFisher), and 10 mM 2-mercaptoethanol (Gibco). Cells were cultured at 37 °C in a humidified incubator with 5% CO_2. 1.000 U ml^{-1} ESGRO leukemia inhibitory factor (LIF, Millipore) was for maintaining ESCs self-renewal. Before seeding, culture dishes were coated with 0.2% gelatin (Sigma-Aldrich) for 30 min. Lithium chloride (Sigma-Aldrich) was used as Li^+ source for all the experiments.

ESC Viability and Proliferation in the Presence of Different Lithium Concentrations: The cells were cultured on gelatin-coated plates to study the role of Li^+ in ESC proliferation and viability at 10.000 cells cm^{-2} in BM supplemented with either different Li^+ concentrations or 1.000 U ml^{-1} of LIF for 3 days. After 1 and 3 days, the ESCs were lysed by Tris/Triton X100/ ethylenediaminetetraacetic acid tetrasodium salt dehydrate (EDTA) (10 mM Tris pH 8, 0.5% Triton X100, 1 mM EDTA) buffer, and proliferation was calculated by quantifying total DNA concentration by a Quant-iT PicoGreen dsDNA Assay Kit (ThermoFisher).

Hemogenic Endothelium Differentiation Experiment: In order to assess Li^+-mediated differentiation of ESCs into HE, the ESCs were cultured at 10.000 cells cm^{-2} on gelatin-coated plates for 6 days in BM and BM supplemented with 2 and 10 mM Li^+. After the first 3 days of culture, the cells were passaged and then sub-cultured for another 3 days.

After 6 days of culture, the HB-like cells developed from ESCs were characterized. HB cells were then matured to HE replacing BM with a maturation medium (N2B27) consisting of DMEM/F12 (Sigma-Aldrich) supplemented with N-2 (Thermofisher), B27 (Thermofisher) supplements, 1% L-glutamine, 0.05% of bovine serum albumin (BSA, Sigma-Aldrich), and 1% P/S, without added Li^+. Cells were cultured in these maturation conditions for an additional 11 days.

Immunofluorescence: Cells were fixed in 4% formaldehyde for 20 min at room temperature (RT), followed by three washes with tris buffered saline (TBS). Samples were blocked with TBS/Triton X100 0.1%/BSA 2% for 1 h at RT and incubated with primary antibodies (Table S1, Supporting Information) overnight at 4 °C. Samples were washed and subsequently incubated with secondary antibodies (Table S1, Supporting Information) for 1 h at RT. Hoechst (dilution 1:7.000, Sigma-Aldrich) was used for nuclear staining. Samples were mounted with 85% glycerol. A Nikon Eclipse i80 fluorescence microscope was used for cell imaging, and protein staining was quantified by image analysis on ImageJ software.

Western Blot Experiments: Cells were lysed in lysis buffer (150 mM NaCl, 50 mM Tris pH 8, 1% Nonidet P-40, 0.5% deoxycholate, 0.1% SDS, 0.2 mM EDTA) supplemented with protease inhibitor cocktail tablets (Roche). Protein samples were boiled in loading buffer (Bio-Rad) for 5 min. Samples were resolved using Mini-PROTEAN Electrophoresis System (Bio-Rad) and transferred to PVDF (GE-Healthcare) membranes by Trans-Blot Semi-Dry Transfer Cell (Bio-Rad). Before immunodetection, membranes were blocked with 5% BSA (Sigma-Aldrich) in TBS/0.1% Tween 20 (Sigma-Aldrich) for 1 h and incubated with primary antibodies (Table S2, Supporting Information) diluted in TBS, 0.1% Tween 20, and 3% BSA overnight at 4 °C. Membranes were washed and incubated with HRP-linked secondary antibody (Table S2, Supporting Information) for 1 h at RT. Proteins were developed by ECL-Plus reactive (ThermoFisher). A Fujifilm Las-3000 imager device was used to visualize the protein bands.

Chromatin Immunoprecipitation: Chromatin immunoprecipitation (ChIP) was performed as previously described (Strahl-Bolsinger et al., 1997). Briefly, cells were fixed for 15 min in 1% formaldehyde, and the reaction was stopped by adding 125 mM glycine (Sigma-Aldrich). After cell lysis, cell extracts were sonicated in a Bandelin Sonoplus Mini 20, using six pulses of 10 s (30% amplitude). Immunoprecipitation was performed using protein G Dynabeads (ThermoFisher) pre-adsorbed with anti β-catenin antibody (ThermoFisher).

Gene Expression Experiments: Whole RNA was isolated by a Quick RNA Miniprep kit (ZYMO Research) and quantified by a Q3000 microvolume spectrophotometer (Quawell). RNAs were retrotranscribed on a Maxima First Strand cDNA Synthesis Kit with Thermolabile dsDNase (ThermoFisher). Real-time quantitative polymerase chain reaction (qPCR) was carried out using the PowerUp SYBR Master Mix (Thermofisher) and 7500 Fast Real-Time PCR System (ThermoFisher). Gene expression was quantified by the $\Delta\Delta$Ct method (Pfaffl, 2001). Sample values were normalized to the threshold value of housekeeping gene GAPDH.

Chromatin immunoprecipitated fragments were amplified by AmpliTaq Gold 360 DNA Polymerase (ThermoFisher) using PTC-1148 MJ Mini Thermal Cycler (Bio-Rad).

The primers used for amplification are indicated in Tables S3 and S4, Supporting Information.

Statistical Analysis: Statistical differences were analyzed by Student's *t*-test and ANOVA using GraphPad Prism 6.0. When differences were determined to be significant, pairwise comparisons were made by the Tukey test in cases of normal data distribution or Dunn's test in the opposite case. A 95% confidence level was considered significant.

Supporting Information

Supporting Information is available from the Wiley Online Library or from the author.

Acknowledgements

P.R. acknowledges support from the Spanish Ministry of Science, Innovation, and Universities (RTI2018-096794), and Fondo Europeo de Desarrollo Regional (FEDER). CIBER-BBN was an initiative funded by the VI National R&D&I Plan 2008–2011, Iniciativa Ingenio 2010, Consolider Program, CIBER Actions and financed by the Instituto de Salud Carlos III with assistance from the European Regional Development Fund. M.S.-S. acknowledges support from the UK Engineering and Physical Sciences Research Council (EPSRC – EP/P001114/1).

Conflict of Interest

The authors declare no conflict of interest.

Data Availability Statement

Data available on request due to privacy/ethical restrictions. The data that support the findings of this study are available on request from the corresponding author. The data are not publicly available due to privacy or ethical restrictions.

Keywords

differentiation, hematopoietic stem cell precursors, lithium, pluripotent stem cells

Received: November 26, 2020
Revised: April 20, 2021
Published online: May 9, 2021

[1] K. Chotinantakul, W. Leeanansaksiri, *Bone Marrow Res.* **2012**, *2012*, 1.
[2] A. P. Ng, W. S. Alexander, *Cell Death Discovery* **2017**, *3*, 17002.
[3] M. Ackermann, S. Liebhaber, J. Klusmann, N. Lachmann, *EMBO Mol. Med.* **2015**, *7*, 1388.
[4] K. K. Hirschi, *Blood* **2012**, *119*, 4823.
[5] G. Swiers, C. Rode, E. Azzoni, M. F. T. R. De Bruijn, *Blood Cells, Mol., Dis.* **2013**, *51*, 206.
[6] C. Lancrin, P. Sroczynska, A. G. Serrano, A. Gandillet, C. Ferreras, V. Kouskoff, G. Lacaud, *J. Mol. Med.* **2010**, *88*, 167.
[7] I. I. Slukvin, *FEBS Lett.* **2016**, *590*, 4126.
[8] C. M. Sturgeon, A. Ditadi, G. Awong, M. Kennedy, G. Keller, *Nat. Biotechnol.* **2014**, *32*, 554.
[9] X. Lian, C. Hsiao, G. Wilson, K. Zhu, L. B. Hazeltine, S. M. Azarin, K. K. Raval, J. Zhang, T. J. Kamp, S. P. Palecek, *Proc. Natl. Acad. Sci. U. S. A.* **2012**, *109*, E1848.
[10] D. Wu, W. Pan, *Trends Biochem. Sci.* **2010**, *35*, 161.
[11] S. S. D'Souza, J. Maufort, A. Kumar, J. Zhang, K. Smuga-Otto, J. A. Thomson, I. I. Slukvin, *Stem Cell Rep.* **2016**, *6*, 243.
[12] L. Freland, J.-M. Beaulieu, *Front. Mol. Neurosci.* **2012**, *5*, 1.
[13] M. M. Schmidt, K. Guan, A. M. Wobus, *Int. J. Dev. Biol.* **2001**, *45*, 421.
[14] T. Chen, F. Wang, M. Wu, Z. Z. Wang, *J. Cell. Biochem.* **2015**, *116*, 1179.
[15] N. Esiashvili, M. A. Pulsipher, in *Pediatric Radiation Oncology* (Eds: T. Merchant, R. D. Kortmann), Springer, Switzerland **2018**, pp. 301–311.
[16] A. Eliades, S. Wareing, E. Marinopoulou, M. Z. H. Fadlullah, R. Patel, J. B. Grabarek, B. Plusa, G. Lacaud, V. Kouskoff, *Cell Rep.* **2016**, *15*, 2185.
[17] M. S. Allagui, C. Vincent, A. E. feki, Y. Gaubin, F. Croute, *Biochim. Biophys. Acta, Mol. Cell Res.* **2007**, *1773*, 1107.
[18] H. M. Zhang, J. Yuan, P. Cheung, D. Chau, B. W. Wong, B. M. McManus, D. Yang, *Mol. Cell. Biol.* **2005**, *25*, 6247.
[19] C. D. Mao, P. Hoang, P. E. DiCorleto, *J. Biol. Chem.* **2001**, *276*, 26180.
[20] A. Raggioli, D. Junghans, S. Rudloff, R. Kemler, *PLoS One* **2014**, *9*, e86691.
[21] Y. Chen, K. Blair, A. Smith, *Stem Cell Rep.* **2013**, *1*, 209.
[22] E. Beurel, S. F. Grieco, R. S. Jope, *Pharmacol. Ther.* **2015**, *148*, 114.
[23] R. L. Clarke, A. D. Yzaguirre, Y. Yashiro-Ohtani, A. Bondue, C. Blanpain, W. S. Pear, N. A. Speck, G. Keller, *Nat. Cell Biol.* **2013**, *15*, 502.
[24] G. Lacaud, L. Gore, M. Kennedy, V. Kouskoff, P. Kingsley, C. Hogan, L. Carlsson, N. Speck, J. Palis, G. Keller, *Blood* **2002**, *100*, 458.
[25] M. J. Chen, Y. Li, M. E. De Obaldia, Q. Yang, A. D. Yzaguirre, T. Yamada-Inagawa, C. S. Vink, A. Bhandoola, E. Dzierzak, N. A. Speck, *Cell Stem Cell* **2011**, *9*, 541.
[26] A. D. Yzaguirre, N. A. Speck, *Dev. Dyn.* **2016**, *245*, 1011.
[27] G. Martello, T. Sugimoto, E. Diamanti, A. Joshi, R. Hannah, S. Ohtsuka, B. Göttgens, H. Niwa, A. Smith, *Cell Stem Cell* **2012**, *11*, 491.
[28] L. Zamir, R. Singh, E. Nathan, R. Patrick, O. Yifa, Y. Yahalom-Ronen, A. A. Arraf, T. M. Schultheiss, S. Suo, J. D. J. Han, G. Peng, N. Jing, Y. Wang, N. Palpant, P. P. L. Tam, R. P. Harvey, E. Tzahor, *Elife* **2017**, *6*, 1.
[29] H. Akazawa, I. Komuro, *Pharmacol. Ther.* **2005**, *107*, 252.
[30] C. O. Lizama, J. S. Hawkins, C. E. Schmitt, F. L. Bos, J. P. Zape, K. M. Cautivo, H. B. Pinto, A. M. Rhyner, H. Yu, M. E. Donohoe, J. D. Wythe, A. C. Zovein, *Nat. Commun.* **2015**, *6*, 7739.
[31] M. J. Chen, T. Yokomizo, B. M. Zeigler, E. Dzierzak, N. A. Speck, *Nature* **2009**, *457*, 887.
[32] I. Kim, T. L. Saunders, S. J. Morrison, *Cell* **2007**, *130*, 470.
[33] M. A. Hanif, H. N. Bhatti, M. A. Ali, M. Asgher, I. A. Bhatti, *Asian J. Chem.* **2010**, *22*, 335.